RSC Advances

ROYAL SOCIETY OF CHEMISTRY

www.rsc.org/advances

RSC Advances

COMMUNICATION

A pyrene-based optical probe capable of molecular computation using chemical input strings

Received 00th January 20xx,
Accepted 00th January 20xx

DOI: 10.1039/x0xx00000x

www.rsc.org/

Megha Chhatwal,[a] Anup Kumar,[a] Rinkoo D. Gupta,*[b] and Satish K. Awasthi*[a]

A pyrene-based optical probe for the real-time and regenerative detection of Cu^{2+} and Fe^{3+} at parts-per-million (ppm) levels is demonstrated. Moreover, the quantifiable changes in the fluorescence signal induced by chemical inputs *viz.* Cu^{2+}, Fe^{3+}, H^+ and CN^- have been exploited to assemble sequential and "four-input" combinatorial molecular logic circuits. A unique "two-way" security lock has also been devised for enhanced information protection at molecular level.

Multi-stimuli responsive[1] "smart molecules" illustrate huge promises in the field of molecular computing. The perturbations caused in their immediate environment by the external stimuli (chemical, electrical and/or optical inputs) get amplified to the macroscopic level in terms of measurable signals (mechanical, optical and/or electrochemical outputs), which can be ingeniously harnessed for Boolean algebraic computations allowing information processing and storage at the molecular level.[2] Chemosensors endowed with a pyrene moiety as the signalling unit generate either emission enhancement or quenching as the output in response to metal ion stimuli.[3] In this context, we introduce a simple pyrene-based probe **1**, for the detection of Cu^{2+}, Fe^{3+} and H^+ ions via discernible colour changes and discriminating emission "turn-off" behaviour. The **1-Cu^{2+}/Fe^{3+}** ensembles could further recognize highly toxic cyanide ion with simultaneous regeneration of probe **1**. Furthermore, these ions (Cu^{2+}, Fe^{3+}, H^+ and CN^-) have been utilized as the input strings to construct molecular-level logic circuits while accessing quantum yield responses as outputs. To the best of our knowledge, there has been no report on any such pyrene-based chemosensor for recognition of all the four ions *viz.* Cu^{2+}, Fe^{3+}, CN^- and H^+ on a single platform, till date.[4]

[a] *Chemical Biology Laboratory, Department of Chemistry, University of Delhi, Delhi-110 007, India*
E-mail: skawasthi@chemistry.du.ac.in
[b] *Faculty of Life Sciences and Biotechnology*
South Asian University
New Delhi-110 021, India.
† *Dedicated to Late Dr. Tarkeshwar Gupta*
Electronic Supplementary Information (ESI) available: [experimental details, characterization and sensing methodology]. See DOI: 10.1039/x0xx00000x

Probe **1** (Scheme 1) has been synthesized in good yield (~70%) by adopting a simple synthetic method[5] and well-characterized using a full-battery of physico-chemical techniques (Fig. S1-S4). The availability of the carbonyl oxygen and pyridine nitrogen atoms makes our probe an enticing receptor for Cu^{2+}, Fe^{3+} and H^+ ions. The probe displays metal/H^+-ion induced differential optical responses (UV-vis and emission) along with contrasting colour changes.

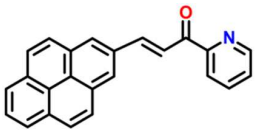

Scheme1. Chemical structure of probe **1**

The UV-vis spectrum of **1** (10^{-5} M, $CHCl_3$) displays an intense peak at λ = 270 nm (ε = 37,000 M^{-1} cm^{-1}) and a broad doublet at λ = 392 nm (ε = 23,000 M^{-1} cm^{-1}) and 430 nm (ε = 26,000 M^{-1} cm^{-1}). However, the spectrum shows immediate perturbations in the presence of Cu^{2+} and Fe^{3+} ions at ppm level concentration associated with visible colour changes from yellow to purple and blue, respectively (Fig. S5-S6). Upon gradual addition of Cu^{2+} (1-20 ppm, CH_3CN) to **1** (10^{-5} M, $CHCl_3$), a moderate hypochromic shift at λ = 430 nm ("turn-off", ΔA = 0.103) coupled with appearance of a new peak at λ = 567 nm ("turn-on", ΔA = 0.352) was observed. Also, two isosbestic points at λ = 370 and 450 nm indicate the formation of **1-Cu^{2+}** ensemble (Fig. 1a). Strikingly, addition of only a small concentration of Fe^{3+} (1-5 ppm, CH_3CN) induced a significant hypochromic shift at λ = 430 nm ("turn-off", ΔA = 0.188) together with an emergence of a broad band with dual peaks at λ = 540 ("turn-on", ΔA = 0.125) and 611 nm ("turn-on", ΔA = 0.128). An isosbestic point at λ = 466 nm accounts for the binding of Fe^{3+} with **1** (Fig. 1b). The spectral responses saturated at 20 ppm and 5 ppm for Cu^{2+} and Fe^{3+}, respectively and no further remarkable changes were detected on increasing the concentration of analytes by two-fold.

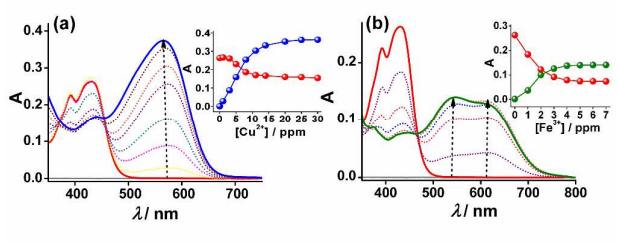

Figure 1. Absorbance changes in **1** (10^{-5} M, $CHCl_3$) (red solid line) upon addition of (a) 20 ppm of Cu^{2+} (blue solid line) and (b) 5 ppm of Fe^{3+} (olive solid line) in CH_3CN. The dotted arrows serve guide to the eyes. Insets: Plot of absorbance at λ = 430 nm (red spheres), 567 nm (blue spheres) and 540 nm (olive spheres) as a function of ppm concentration of Cu^{2+} and Fe^{3+}.

Furthermore, probe **1** is an intense luminophore (ϕ_f = 0.62, using anthracene as standard) and exhibits an emission peak at λ = 520 nm (λ_{ex} = 270 nm). Plausibly, the peak can be assigned to intermolecular excimer emission due to π-π stacking of pyrene units.[3a] Interestingly, upon addition of 20 ppm of Cu^{2+} (~8.3 equiv.), **1** showed "turn-off" emission response with I_0/I = ~7 ($\phi_{f(1\text{-}Cu^{2+})}$ = 0.09) and a miniscule concentration of 5 ppm (~3.1 equiv.) of Fe^{3+} also led to diminishing of the emission peak with I_0/I = ~13 ($\phi_{f(1\text{-}Fe^{3+})}$ = 0.05) (Fig. 2). The quenching could also be visualized under UV lamp (Fig S7). The fluorescence quenching is attributed to the non-radiative processes caused by paramagnetic effect of unpaired d-electrons of Cu^{2+} (d^9) and Fe^{3+} (d^5).[6] The Stern-Volmer plots were non-linear with an upward curvature indicating both static (collisional) as well as dynamic (formation of non-fluorescent ground state complex) quenching mechanisms operating together (Fig. S8).[7]

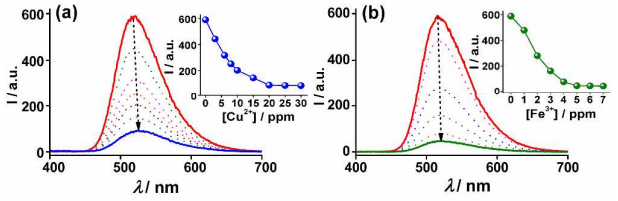

Figure 2. Emission intensity changes in **1** (10^{-5} M, $CHCl_3$) (red solid line) upon addition of (a) 20 ppm of Cu^{2+} (blue solid line) and (b) 5 ppm of Fe^{3+} (olive solid line) in CH_3CN. The excitation wavelength was fixed at λ = 270 nm. The dotted arrows serve guide to the eyes. Insets: Plot of emission intensity at λ = 520 nm as a function of ppm concentration of Cu^{2+} (blue spheres) and Fe^{3+} (olive spheres).

The detection limits of **1** for Cu^{2+} and Fe^{3+} came out to be 4.4 × 10^{-6} M (~1 ppm) and 2.3 × 10^{-6} M (~0.4 ppm), respectively.[8a] The stoichiometric ratio of 2:1 for both **1-Cu^{2+}** and **1-Fe^{3+}** couples was evaluated from Job's method of continuous variation of mole-fraction (Fig. S9). The binding ratio has also been confirmed by ESI-MS data. A clear peak at *m/z* = 729.79 may be attributed to the fragment [2.probe1 + Cu] (calc. *m/z* = 729.16) (Fig. S10) and a peak at *m/z* = 304.86 most likely corresponds to the fragment [2.probe1 + $Fe(CH_3CN)_2.6H_2O]^{3+}$ (calc. *m/z* = 304.09) (Fig. S11). The binding constants computed from Benesi-Hildebrand plots assuming 2:1 molecular arrangement were 1.72 × 10^2 $M^{-1/2}$ and 1.94 × 10^3 $M^{-1/2}$ for Cu^{2+} and Fe^{3+}, respectively (Fig. S12).[8b]

An excellent probe needs to demonstrate highly selective identification in the competitive environment of analytes. The chemosensor **1** exclusively detects Cu^{2+} and Fe^{3+} over a wide range of other metal ions. No other metal ion could produce any remarkable change in the emission spectra of **1** (red bars). Furthermore, quenching efficiency of the probe for Cu^{2+} (blue bars) and Fe^{3+} (olive bars) ions was not deterred even by the presence of other test stimuli in a matrix arrangement (Fig. 3). Apparently due to its higher binding constant, Fe^{3+} most likely replaces Cu^{2+} from **1-Cu^{2+}** couple further decreasing the emission intensity (blue bars, entry 17, Fig 3a).

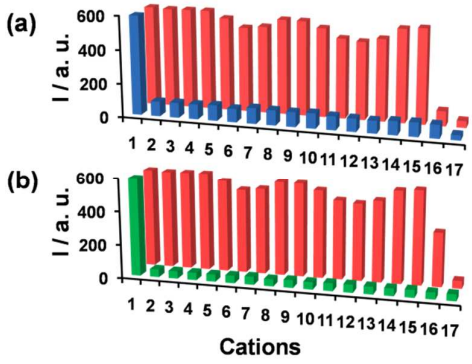

Figure 3. Representative bar chart showing emission intensity responses at λ = 520 nm upon addition of (a) 20 ppm of test metal analytes in **1** (10^{-5} M, $CHCl_3$) (red bars) and **1-Cu^{2+}** solution (blue bars); (b) 5 ppm of test metal analytes in **1** (10^{-5} M, $CHCl_3$) (red bars) and **1-Fe^{3+}** solution (olive bars). 1 = None, 2 = Na^+, 3 = Mg^{2+}, 4 = Ca^{2+}, 5 = Mn^{2+}, 6 = Fe^{2+}, 7 = Co^{2+}, 8 = Ni^{2+}, 9 = Zn^{2+}, 10 = Ag^+, 11 = Cd^{2+}, 12 = Hg^{2+}, 13 = Pb^{2+}, 14 = Al^{3+}, 15 = Cr^{3+}, 16 = Cu^{2+} and 17= Fe^{3+}.

Recyclability of a chemosensor is crucial for cost-effective real-sample measurements. Addition of 5 ppm of CN^- (in ethanol) in the respective solutions of **1-Cu^{2+}** and **1-Fe^{3+}** complexes, not only reverted back the emission intensity of probe **1** but also brought back its initial yellow colour (Fig. 4a). This possibly implies sequestering of Cu^{2+} and Fe^{3+} by CN^- to potentially form $[Cu(CN)_x]^{n-}$ and $[Fe(CN)_x]^{n-}$, releasing probe **1** in the solution.[9] None of the other investigated anions could remarkably raise the quenched fluorescence signal (Fig. 4b). Both **1-Cu^{2+}** and **1-Fe^{3+}** systems showed good on/off ratio for at least three cycles with only a minimal signal loss of ~9% and ~19%, respectively (Fig. S13). It is noteworthy to mention here, that probe **1** depicted an added advantage of detection of a potentially toxic stimulus (CN^-).

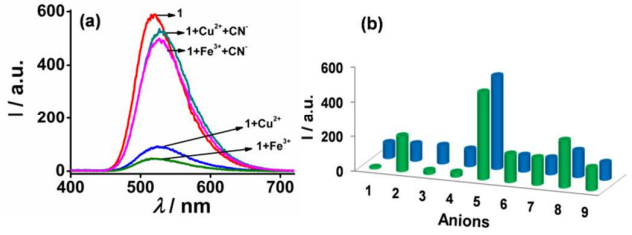

Figure 4. (a) Regeneration of emission intensity of **1-Cu^{2+}/Fe^{3+}** (**1** + 20 ppm Cu^{2+} / 5 ppm Fe^{3+}) upon addition of 5 ppm of CN^- (in EtOH); (b) Representative bar chart showing the effect of addition of 5 ppm of various anions in the solution of **1-Cu^{2+}** (blue bars) and **1-**

Fe^{3+} (olive bars). 1 = None, 2 = Br^-, 3 = Cl^-, 4 = I^-, 5 = CN^-, 6 = PF_6^-, 7 = SCN^-, 8 = F^- and 9 = ClO_4^-.

Another feather in our probe's cap is its distinct optical response towards the presence of H^+ ions. Upon gradual addition of H^+ ions (0.3 mM to 2 mM, CH_3CN) to the solution of **1** (10^{-5} M, $CHCl_3$), a new absorption band arises at λ = 488 nm ("turn-on", ΔA = 0.313) along with fading of the original bands. This could be ascribed to the protonation of pyridine nitrogen atom. The response was visually detectable with a colour change from yellow to orange. On the other hand, the emission peak plummets (I_0/I = ~3.5, $\phi_{f(1\text{-}H^+)}$ = 0.18) coupled with the shifting of λ_{max} to 550 nm (bathochromic shift of ~30 nm) as H^+ ions (0.04 mM to 2 mM, CH_3CN) are introduced into the system (Fig 5).

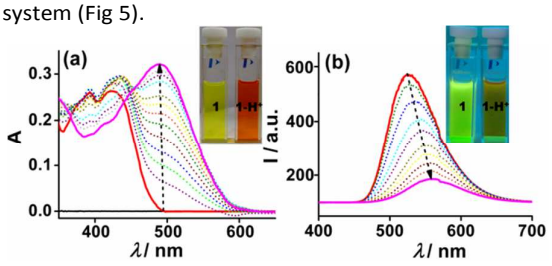

Figure 5. (a) Absorbance and (b) emission intensity changes in **1** (10^{-5} M, $CHCl_3$) (red solid line) upon addition of H^+ (2 mM, CH_3CN) (pink solid line). The dotted arrows serve guide to the eyes. Insets: Photographs depicting the colour change and fluorescence quenching in **1** upon addition of H^+.

As explained, probe **1** acts as an "ON-OFF-ON" fluorescent switch controlled by Cu^{2+}/Fe^{3+} and CN^- ions (*vide supra*). The set-reset of probe **1** by these stimuli can process information in the form of two-input sequential and combinatorial logic circuits.[10] The variations in the quantum yield at λ = 520 nm have been captured as outputs and the threshold has been fixed at ϕ_f = 0.3. The sequential logic circuit is designed in such a way that Cu^{2+} ion behaves as IN1 whereas CN^- ion functions as IN2 (Fig. 6a). When IN1 is high, the quantum yield falls below the threshold level to give OUT = 0 and the stored information is "erased" from the system. However, subsequent addition of IN2 again "writes" the information in the system as it regains its initial quantum yield with OUT = 1. The feedback loop connects the output back to IN1 and ensures memory function of the circuit. When the sequence order of the inputs is reversed and CN^- ion (IN1) is added before Cu^{2+} ion (IN2), a combinatorial logic circuit mimicking the functions of NOT, AND and OR gates, is obtained (Fig. 6b). In this case, already present CN^- ions (IN1 = 1) in the system could not sequester the metal ion (IN2 = 1) and thus, the information is "read" in terms of low output (OUT = 0). These logic systems could also be concatenated for Fe^{3+} ion.

Evidently, the above used input events are order dependent and generate TRUE output only when addition of Cu^{2+}/Fe^{3+} precedes that of CN^-. Hence, the system more or less behaves like a priority AND gate. This modulation in the input sequence could also be realised to devise a miniaturized "two-way" security lock[11] for information cascade at molecular level. The inputs Cu^{2+}, Fe^{3+} and CN^- ions are coded as "U", "S" and "B", respectively. Out of six possible combinations (USB, BSU, SBU, UBS, SUB and BUS), the input sequence "USB" unlocks the emission signal at λ = 520 nm.

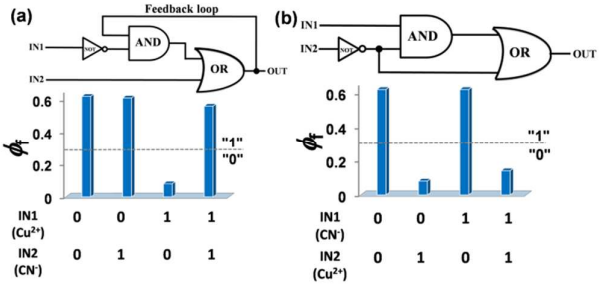

Figure 6. Quantum yield outputs of **1** at λ = 520 nm in the presence of chemical inputs *viz.* (a) IN1 = Cu^{2+}, IN2 = CN^- along with the corresponding two-input sequential logic circuit, and (b) IN1 = CN^-, IN2 = Cu^{2+} along with the corresponding two-input combinatorial logic circuit. Dotted lines represent the threshold level. The output above the threshold level is read as "1" otherwise "0".

Markedly, the positions of inputs "U" and "S" could be dexterously interchanged with each other to generate another input sequence "SUB" which could also turn-on the emission signal. Thus, this "joint molecular account" is held by two authorized users who equally share the right to activate the emission channel by entering their respective coded sequence of keys (either "USB" or "SUB"). Any other key string, if pressed would fail to open the lock and produce an alarm (FALSE) signal. (Fig. 7).

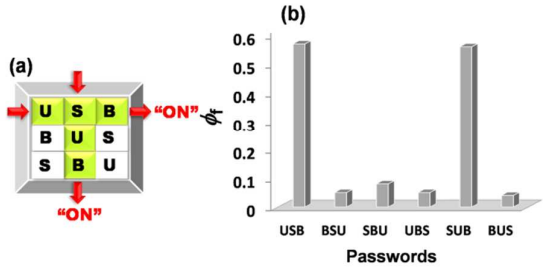

Figure 7. (a) Unique "two-way" security lock being accessed (*"ON"*) at λ = 520 nm only by correct sequence of entries (*"USB"* or *"SUB"*). (b) Quantum yield outputs corresponding to six probable input sequences. The keys "U", "S" and "B" hold Cu^{2+}, Fe^{3+} and CN^- as inputs.

Further, sixteen different combinations of four chemical inputs *viz.* Cu^{2+} (IN1), Fe^{3+} (IN2), CN^- (IN3) and H^+ (IN4) were used to address the emission quantum yield outputs at λ = 520 nm (OUT). The threshold has been set at ϕ_f = 0.30. OUT is generated by a combinatorial circuit comprising of NOR, OR and INH gates wired together. (Fig. 8). Therefore, the fluorogenic sensing traits of probe **1** can be usefully extended to configure molecular level logic circuits to store the optical information as encoded by appropriate chemical input signals.

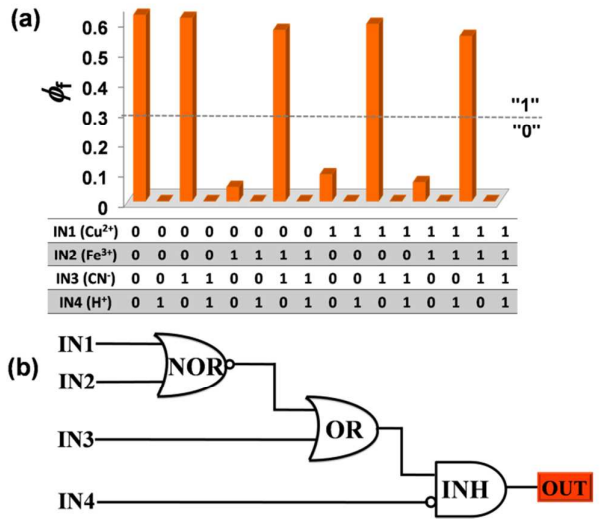

Figure 8. (a) Quantum yield outputs of **1** at λ = 520 nm (OUT) in the presence of chemical inputs *viz.* IN1 = Cu^{2+}, IN2 = Fe^{3+}, IN3 = CN^- and IN4 = H^+. Dotted lines represent the threshold level. The output above the threshold level is read as "1" otherwise "0". (b) The corresponding four-input combinatorial logic circuit.

Conclusions

In conclusion, we have presented a simple pyrene-appended chemosensor for differential monitoring of Cu^{2+}, Fe^{3+} and H^+ ions via distinct colour changes and emission quenching. The **1-Cu^{2+}/Fe^{3+}** couples formed in situ could further detect toxic CN^- ions while reverting the probe **1** back into the solution. Most importantly, the probe adds further impetus to the field of molecular devices while performing Boolean algebraic operations to integrate two-input sequential as well as combinatorial logic circuits by controlling the sequence of input addition. Additionally, a complex four-input combinatorial logic circuit could also be achieved. Thus, probe **1** offers highly selective, sensitive and reversible detection of Cu^{2+} and Fe^{3+} and also opens new avenues to explore the potential of chemosensors as memory elements.

Acknowledgements

RDG thanks DST (SERB/F/1424/2013-14) and South Asian University, New Delhi, India for financial assistance. MC thanks CSIR, India for award of Senior Research Fellowship and University of Delhi for technical support.

Notes and references

1 (a) K. Chen, Q. Shu and M. Schmittel, *Chem. Soc. Rev.*, 2015, **44**, 136; (b) M. Chhatwal, A. Kumar, V. Singh, R. D. Gupta and S. K. Awasthi, *Coord. Chem. Rev.*, 2015, **292**, 30; (c) S. Banthia, A. Samanta, *Eur. J. Org. Chem.,* 2005, 4967.

2 (a) A. P. de Silva and N. D. McClenaghan, *Chem. Eur. J.*, 2004, **10**, 574, (b) J. Andréasson and U. Pischel, *Chem. Soc. Rev.*, 2015, **44**, 1053; (c) A. Credi, *Angew. Chem. Int. Ed.*, 2007, **46**, 5472; (d) J. Andréasson, U. Pischel, *Chem. Soc. Rev.,* 2015, **44**, 1053.

3 (a) C. Kar, M. D. Adhikari, A. Ramesh and G. Das, *RSC Adv.*, 2012, **2**, 9201; (b) L. Ding, S. Wang, Y. Liu, J. Cao and Y. Fang, *J. Mater. Chem.*, 2013, **1**, 8866; (c) T. Raj, P. Saluja, N. Singh, *Sens. Actuators B*, 2015, **206**, 98; (d) M. Kumar, A. Dhir and V. Bhalla, *Eur. J. Org. Chem.*, 2009,4534; (e) M. Kumar, R. Kumar, V. Bhalla, *Tetrahedron Lett.,* 2010, **51**, 5559.

4 (a) E. Manandhar and K. J. Wallace, *Inorg. Chim. Acta.*, 2012, **381**, 15; (b) Y. R. Bhorge, H. Tsaia, K. Huang, A. J. Pape, S. N. Janaki and Y. Yen, *Spectrochim. Acta Part A Mol. Biomol. Spectrosc.*, 2014, **130**, 7; (c) N. Sharma, S. I. Reja, V. Bhalla, M. Kumar, *Dalton Trans.,* 2014, **43**, 15929; (d) M. Wang, J. Xu, X. Liu, H. Wang, *New J. Chem.,* 2013, **37**, 3869.

5 W. Leslie, R. A. Poole, P. R. Murray, L. J. Yellowlees, A. Beeby and J. A. G. Williams, *Polyhedron*, 2004, **23**, 2769.

6 (a) A. W. Varnes, R. B. Dodson and E. L. Wehry, *J. Am. Chem. Soc.*, 1972, **94**, 946; (b) S. K. Sahoo, D. Sharma, R. K. Bera, G. Crisponi and J. F. Callan, Chem. Soc. Rev., 2012, **41**, 7195.

7 J. R. Lakowicz, *Principles of fluorescence spectroscopy, Springer*, New York, 3rd edn, 2006.

8 (a) A. Kumar, M. Chhatwal, R. D. Gupta, S. K. Awasthi, *RSC Adv.*, 2015, **5**, 5217, (b) S. Sarkar, S. Roy, A. Sikdar, R. N. Saha and S. S. Panja, *Analyst*, 2013, **138**, 7119.

9 P. Kaur, H. Kaur and K. Singh, *RSC Adv.*, 2013, **3**, 64.

10 (a) G. de Ruiter, E. Tartakovsky, N. Oded and M. E. van der Boom, *Angew. Chem. Int. Ed.*, 2010, **49**, 169; (b) S. Karmakar, D. Maity, S. Mardanya and S. Baitalik, J. Phys. Chem. A, 2014, **118**, 9397; (c) L. Wang B. Li, L. Zhang and Y. Luo, *Dalton Trans.*, 2013, **42**, 459; (d) M. A. Kaloo and J. Sankar, *New J. Chem.*, 2014, **38**, 923; (e) V. Bhalla, Roopa, M. Kumar, *Dalton Trans.,* 2013, **42**, 13390; (f) M. Kumar, S. I. Reja, V. Bhalla, *Org. Lett.,* 2012, **14**, 6084.

11 (a) D. Margulies, C. E. Felder, G. Melman and A. Shanzer, *J. Am. Chem. Soc.*, 2007, **129**, 347; (b) M. Suresh. A. Ghosh and A. Das, *Chem. Commun.*, 2008, 3906; (c) M Kumar, R Kumar, V Bhalla, *Chem. Comm.,* 2009, 7384; (d) M Kumar, A Dhir, V Bhalla, *Org. Lett.*, 2009, **11**, 2567; (e) Y. Wang, Y. Huang, B. Li, L. Zhang, H. Song, H. Jiang and J. Gao, *RSC Adv.*, 2011, **1**, 1294; (f) V. Bhalla, V. Vij, M. Kumar, P. R. Sharma, and T. Kaur, *Org. Lett.*, 2012, **14**, 1012.

